

## Two-way optical frequency comparisons at $5 \times 10^{-21}$ relative stability over 100-km telecommunication network fibers

Anthony Bercy,<sup>1,2</sup> Fabio Stefani,<sup>2</sup> Olivier Lopez,<sup>1</sup> Christian Chardonnet,<sup>1</sup> Paul-Eric Pottie,<sup>2,\*</sup> and Anne Amy-Klein<sup>1,†</sup>

<sup>1</sup>*Laboratoire de Physique des Lasers, Université Paris 13, Sorbonne Paris Cité, CNRS, 99 Avenue Jean-Baptiste Clément, 93430 Villetaneuse, France*

<sup>2</sup>*Laboratoire National de Métrologie et d'Essais-Systèmes de Référence Temps-Espace, UMR 8630, Observatoire de Paris, CNRS, UPMC, 61 Avenue de l'Observatoire, 75014 Paris, France*

(Received 28 July 2014; published 22 December 2014)

By using two-way frequency transfer, we implement a real-time frequency comparison over a uni-directional telecommunication network of 100 km using a pair of parallel fibers with simultaneous digital data transfer. The relative frequency stability is  $10^{-15}$  at 1-s integration time and reaches  $2 \times 10^{-17}$  at 40 000 s, three orders of magnitude below the one-way fiber instability. We also demonstrate ultrahigh-resolution comparison of optical frequencies with a bidirectional scheme using a single fiber. We show that the relative stability at 1-s integration time is  $7 \times 10^{-18}$  and scales down to  $5 \times 10^{-21}$ . The same level of performance is reached when an optical link is implemented with an active compensation of the fiber noise. The fractional uncertainty of the frequency comparisons was evaluated for the best case to  $2 \times 10^{-20}$ . These results open the way to accurate and high-resolution frequency comparison of optical clocks over intercontinental fiber networks.

DOI: [10.1103/PhysRevA.90.061802](https://doi.org/10.1103/PhysRevA.90.061802)

PACS number(s): 42.62.Eh, 06.20.fb, 06.30.Ft

High-resolution time and frequency transfer between remote locations are of major interest for many applications, such as tests of general relativity and temporal variation of fundamental constants, future redefinition of the second, relativistic geodesy, and navigation (see [1], and references herein). It is usually performed through satellite-based time and frequency transfer but with performance now insufficient for state-of-the-art optical clocks and laser oscillators [2–4]. As a very promising alternative, optical fiber links are intensively studied for a decade by several groups, for frequency transfer [5–10] and for frequency-comb transfer [11]. They demonstrate impressive results far beyond the GPS capabilities on distances up to 1840 km with bidirectional dedicated fibers [12]. Our groups extended the technique of optical link to active telecommunication fiber networks by inserting optical add-drop multiplexers (OADM) in every amplification site and network node. Bidirectional frequency transfer was enabled on one 100-GHz dedicated channel, in parallel with unidirectional data traffic over all the other channels [13]. This technique proved to be very efficient for ultrastable time and frequency transfer on a continental scale [14]. It gives the possibility to disseminate a frequency standard to a wide number of laboratories, for high-resolution spectroscopy, remote laser stabilization, and any high-precision measurements.

If one focuses on optical frequency comparisons, and puts the frequency transfer aside, the setup can be drastically simplified with a two-way method [15]. At each end of the fiber link, a laser is sent to the other end and one detects the frequency difference between the local laser and the remote laser. Assuming that the propagation frequency noise is equal for the two directions of propagation, one can efficiently reject the propagation contributions by synchronizing and postprocessing the data, simply subtracting and

dividing by 2 the two data sets recorded at each end. The in-field implementation of the two-way method requires two ultrastable lasers at each end, and an accurate control of their frequency drifts. This can be done actively by locking the laser frequency to an atomic clock or a maser, or passively by time stamping the data of the frequency measurements in both laboratories [16]. Two-way frequency comparison was recently demonstrated over a 47-km loop in an urban link using a Sagnac interferometer [17]. But the latter imposes the two ends to be in the same place. We consider in this Rapid Communication two alternative two-way schemes which can be practically implemented between distant laboratories and we demonstrate them over a 100-km urban link. One scheme uses a single fiber through which the light is propagated in both directions (from here on referred to as two-way bidirectional or 2WB). It exhibits a very low instability, thanks to the very good rejection of the fiber noise. The other one uses two parallel fibers, each fiber transmitting the light in a single direction (referred to as two-way uni-directional or 2WU) as first proposed by [18]. Despite its higher instability, this unidirectional scheme outperforms satellite comparison techniques for short averaging time. Moreover it opens the way to frequency comparisons over a telecommunication network with minimal modification of the network backbone.

The Rapid Communication is organized as follows: We first describe the two schemes of two-way frequency comparisons we have implemented. Second, we present the experimental results and the extrapolation to long haul links of unidirectional two-way frequency comparisons.

In order to demonstrate in real conditions two-way frequency comparison and to assess its performances, we used a pair of optical fibers forming two parallel loops of 100 km in the Paris area. The loop starts and ends at Laboratoire de Physique des Lasers and is constituted of six fibers spans. In each span, we access two fibers placed in the same cable. Two nonconsecutive spans of 10 and 8 km are active telecommunication fibers from French Research Network

\*paul-eric.pottie@obspm.fr

†anne.amy-klein@univ-paris13.fr

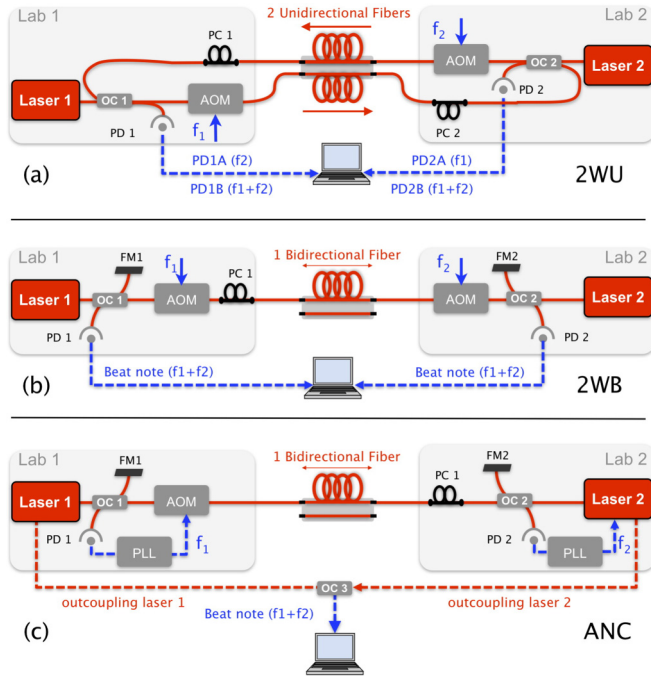


FIG. 1. (Color online) Experimental setups for frequency comparison: (a) two-way unidirectional, (b) two-way bidirectional, and (c) active noise compensated link. AOM, acousto-optic modulator; PC, polarization controller; FM, Faraday mirror; OC, optical coupler; PD, photodiode; PLL, phase lock loop.

(Renater), simultaneously used for data traffic. Eight OADMs are used to insert and to extract the ultrastable signal at  $1.5 \mu\text{m}$  into these spans. The four other spans are dedicated fibers. We installed halfway one erbium-doped fiber amplifier (EDFA) with 20 dB gain on each fiber to partly compensate the 45 dB losses measured on the first fiber. We use two independent detection setups, one at each end, to make the system usable for two distant laboratories, as detailed below.

We have first implemented a two-way method using two fibers and unidirectional propagation. This configuration can be straightforwardly employed on telecommunication networks which are operated this way. The setup is sketched in Fig. 1(a). The left to right and right to left counterpropagating optical signals are propagating into two unidirectional fibers. The frequencies of the two lasers located at each end are shifted with two acousto-optics modulators (AOM) at frequencies  $f_1$  and  $f_2$ , one on each fiber, in order to distinguish the useful signals from parasitic back reflections. At each end, a Michelson-type interferometer is implemented, instead of the circulators of the first proposal [18]. This new configuration enables one to detect two beat notes on the two photodiodes PD1 and PD2 at each end: the beat note between the local and remote lasers, of frequency  $f_1$  or  $f_2$ , labeled as *A*, and the beat note between the local laser with itself after a round-trip in both fibers successively, of frequency  $f_1 + f_2$ , labeled as *B*. The beat notes are optimized with two polarization controllers. Those at frequency  $f_1 + f_2$  are more attenuated because of a double circulation in the loop. Thus a tracking oscillator is phase locked to them with a bandwidth of 100 kHz. After amplification and filtering, the beat note signals are

simultaneously recorded with a gate time of 1 s with two dead-time free frequency counters operated in  $\Pi$  type and  $\Lambda$  type [19].

Let us consider a simplified, steady state model of the two-way phase detected in that configuration. One can write the beat note signals detected by the photodiodes PD1 and PD2 as follows:

$$\begin{aligned} \text{PD1}_A &= (\Phi_2 + \Phi_{21}) - \Phi_1 && \text{at frequency } f_2, \\ \text{PD1}_B &= (\Phi_{12} + \Phi_{21}) && \text{at frequency } f_1 + f_2, \\ \text{PD2}_A &= (\Phi_1 + \Phi_{12}) - \Phi_2 && \text{at frequency } f_1, \\ \text{PD2}_B &= (\Phi_{12} + \Phi_{21}) && \text{at frequency } f_1 + f_2, \end{aligned} \quad (1)$$

where  $\Phi_1$  and  $\Phi_2$  are the phase noises associated with laser 1 and laser 2, and  $\Phi_{12}$  and  $\Phi_{21}$  are the noises added by the two fibers, respectively (independent of the lasers at first order). It can be easily demonstrated that, for any realistic amount of fiber attenuation, the successive loops of light signals are not perturbing the considered measurements. Combining the signals labeled as *A* in Eq. (1) in postprocessing gives

$$(-\text{PD1}_A + \text{PD2}_A)/2 = (\Phi_1 - \Phi_2) + (\Phi_{12} - \Phi_{21})/2. \quad (2)$$

This signal will be referred to as remote two-way unidirectional. Under the assumption that  $\Phi_{12} = \Phi_{21}$ , one finds the standard two-way noise rejection, as the fiber noise cancels out and only the laser's phase difference remains. Assuming that the phase noise of both fibers is partly correlated in this setup, one expects a partial noise cancellation for a frequency comparison. The same results can be obtained by combining the two beat notes of the same photodiode. For instance, on PD1 one has

$$-\text{PD1}_A + \text{PD1}_B/2 = (\Phi_1 - \Phi_2) + (\Phi_{12} - \Phi_{21})/2, \quad (3)$$

and similarly on PD2. This approach, which we called ‘‘local two-way,’’ allows us to process the noise rejection at each distant laboratory, using only data acquired locally. It avoids the necessity to exchange and synchronize data between distant sites to remove the propagation noise. When using the same laser at both ends, the term  $(\Phi_1 - \Phi_2)$  vanished in the above equations and one is only sensitive to the residual uncorrelated fiber's noise.

To reject this uncorrelated fiber's noise, one single fiber has to be used for the two counterpropagating signals. In order to study this noise rejection, we tested a two-way bidirectional configuration [see Fig. 1(b)]. The setup is similar to that of the 2WU, with two AOMs at frequencies  $f_1$  and  $f_2$  and two Michelson-type interferometers, one at each end of the single fiber. A single polarization controller is used to optimize the beat notes. With this setup we detect on each photodiode a single beat note between the local and remote lasers, at frequency  $f_1 + f_2$ . After detection, amplification, and filtering, the two end's beat notes are simultaneously counted and processed to obtain the optical frequency comparison, as with the 2WU setup.

Following the general approach of [5], we can derive the residual expected noise of this bidirectional two-way setup [17]. Its origin is similar to that of the delay-unsuppressed noise in a noise compensated link. The total one-way phase perturbation  $\Phi_{12}$  ( $\Phi_{21}$ , respectively) arising for the signal

propagating from Lab1 to Lab2 (see Fig. 1) (from Lab 2 to Lab 1, respectively) reads  $\Phi_{12}(t) = \int_0^L \delta\varphi(z, t - \frac{L-z}{v}) dz$  and  $\Phi_{21}(t) = \int_0^L \delta\varphi(z, t - z/v) dz$ , where  $v$  is the light celerity in the fiber,  $L$  the loop length, and  $\delta\varphi$  the phase perturbation per unit of length at coordinate  $z$  at time  $t$ . For slow variation of the phase noise per unit of length compared to the round-trip time, the two-way phase  $\Phi_{\text{tw}(t)} = 1/2 [\Phi_{12}(t) - \Phi_{21}(t)]$  can be derived at first order as

$$\Phi_{\text{tw}(t)} = \frac{1}{2} \int_0^L \frac{\partial \delta\varphi(z, t)}{\partial t} \left( \frac{2z - L}{v} \right) dz. \quad (4)$$

The two-way phase noise power spectral density (PSD) of this signal is calculated as the Fourier transform of its autocorrelation function,  $R_{\text{tw}}(\tau) = \overline{\Phi_{\text{tw}}(t)\Phi_{\text{tw}}(t + \tau)}$  [20]. Assuming that the fiber noise per unit of length is uncorrelated in position and has constant statistical properties over  $z$  [20], one obtains

$$S_{\Phi_{\text{tw}}}(\omega) = S_{\Phi_{12}}(\omega) \frac{[2\pi f(L/v)]^2}{12}, \quad (5)$$

where  $S_{\Phi_{12}}(\omega)$  is the one-way phase noise PSD expressed in  $\text{rad}^2/\text{Hz}$ . This formula is very similar to that obtained for an optical link with active noise compensation, but with a factor 1/12 instead of 1/3, since the two-way phase is half of the difference between the one-way phase signals [5,17]. It gives an additional rejection factor of 1/4 for the two-way bidirectional setup.

In order to check this statement, we set up on the same 100-km fiber loop an active noise compensated link [see Fig. 1(c)] referred to as ANC later on [21], and recorded the beat note between the two ends of the link at the same frequency  $f_1 + f_2$ . A noticeable change is that the fiber laser is then phase locked to an ultrastable laser, itself locked to an ultrastable cavity, transferred from SYRTE to LPL on a 43-km-long dedicated fiber [22].

We assess the ultimate performances of the two-way setups by injecting both ends with a single fiber laser. For each setup, the two interferometers are hosted in a single, thermally controlled box. They are carefully designed, so that most of the interferometer noise is rejected [23].

We first derive the relative frequency stability of the frequency comparisons, expressed as the modified Allan deviation (MDEV) [19]. Figure 2 displays these stabilities for the one-way fiber noise [green up triangles (a)], the remote 2WU [blue rounds (b)], the local 2WU [red squares (c)], and the 2WB [black diamonds (e)]. For both configurations, we did not suppress any point from the data sets. The local two-way unidirectional stability is as low as  $10^{-15}$  at 1 s integration time and reaches  $2 \times 10^{-17}$  at 40 000 s. The remote 2WU has almost the same performance. This demonstrates the excellent capabilities of 2WU for frequency comparison of the best atomic fountain clocks. This level of performance is indeed already far beyond the most advanced global positioning system (GPS) and two-way carrier phase capabilities [4]. The two-way bidirectional stability is as low as  $7 \times 10^{-18}$  at 1 s and reaches  $5 \times 10^{-21}$  at 4000 s, which is one of the best frequency comparison stabilities reported so far in a very noisy urban environment. For averaging times longer than 100 s, it is limited by the noise floor [brown down triangles (f)]. We

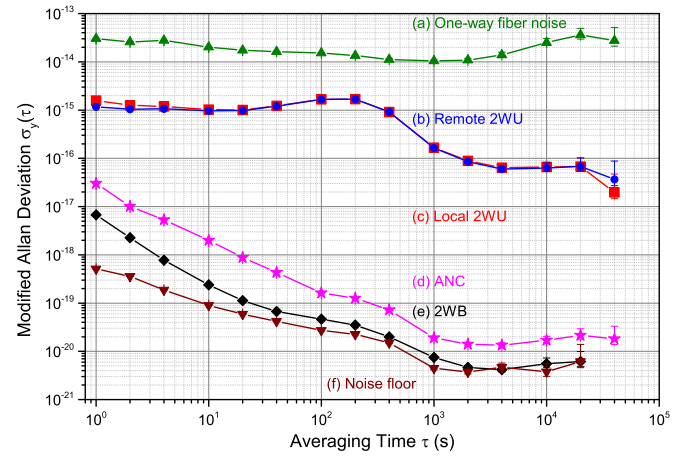


FIG. 2. (Color online) Fractional frequency instability derived from data recorded with  $\Lambda$  counter and expressed as the modified Allan deviation for (a) one-way fiber noise, (b) two-way unidirectional as reconstructed from data recorded at the two ends, (c) local two-way unidirectional, (d) active noise compensated link, (e) two-way bidirectional, and (f) two-way bidirectional noise floor. The other noise floors are similar and are not shown for the sake of clarity.

also plot in Fig. 2 the stability of an ANC link using the same 100-km fiber loop [pink stars (d)]. The 2WB relative stability is about four times below that of the ANC setup, which is more than expected.

To further investigate the noise rejection of the three setups sketched in Fig. 1, we plot in Fig. 3 their phase noise PSDs. The measurements were done using a frequency counter with a gate time of 1 ms and  $\Pi$ -type operation. Frequency data were converted to phase data. Referring to Eq. (5) and [5], the ANC PSD was scaled by a factor 1/4 (i.e., 6 dB) in order to make the comparison with the two-way PSDs easier. The two upper curves in Fig. 3 are the noise PSDs of the one-way [orange curve (a)] and the free-running fiber noise [green curve (b)], the latter being measured with the

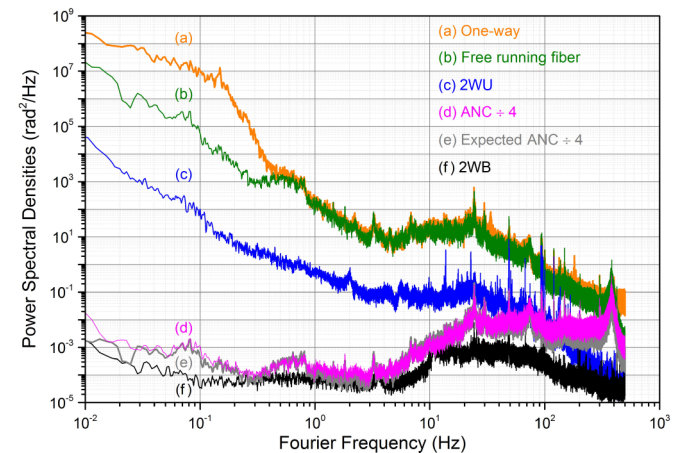


FIG. 3. (Color online) Phase noise PSD for the three setups of Fig. 1. 1 s: (a) one-way, (b) free-running fiber noise for the ANC setup, (c) two-way unidirectional, where real-time and post-processed overlapped themselves, (d) active noise compensation ( $\div 4$ ), (e) expected ANC ( $\div 4$ ), and (f) two-way bidirectional.

ANC setup using a frequency-stabilized laser. The one-way PSD exhibits an excess noise compared to the free-running fiber noise for  $f < 5 \times 10^{-1}$  Hz, which is due to the noise of the unstabilized laser used for the two-way setups. This common noise source for the two counterpropagating signals is well rejected with the two-way setups. The 2WU PSD [blue curve (c)] is about two orders of magnitude below the free-running fiber noise, demonstrating a significant rejection of the propagation noise. The 2WB PSD is at a very low level of around  $6 \times 10^{-5}$  rad<sup>2</sup>/Hz between 0.1 and 60 Hz. Although showing a similar behavior, it is below the scaled ANC PSD [pink curve (d)], when both curves were expected to coincide from the theoretical prediction. We checked that the ANC PSD was overlapping with the expected unsuppressed noise [gray curve (e)] calculated from the free-running fiber noise [5,20]. Thus the discrepancy between the ANC and 2WB noise PSDs may result from an overcorrection in the 2WB setup. This rejection anomaly shows that the assumptions we made on Eq. (4), and on homogeneous noise and uncorrelated noise in position, are violated at some point. In an urban area network, we are indeed observing greater acoustic noise compared to optical links deployed in field. Such acoustic noise is correlated for the two ends of the fiber, since they are located in the same laboratory and follow parallel paths inside the university. It can thus be rejected with the two-way setup. Further investigations are needed on the noise correlation properties to corroborate this point.

We now extrapolate our result on 2WU frequency comparison to an 800-km link, connecting Paris to London, for instance. We are expecting that the stability is limited by the uncommon fiber noise, which we assume homogeneous with a deviation scaling as  $\sqrt{L}$ . We thus calculate a MDEV of  $4 \times 10^{-15}$  at 1 s and  $9 \times 10^{-17}$  at 30 000 s integration time. When considering a transatlantic link, one has to take into account that the noise deviation of a submarine link is about 10 times smaller [24]. For a link constituted of a 6500-km submarine link and a 1000-km terrestrial link, we obtained an expected MDEV of  $5 \times 10^{-15}$  at 1 s and  $1 \times 10^{-16}$  at 30 000 s integration time, dominated by the terrestrial noise. We checked that the delay unsuppressed noise, scaling as  $L^{3/2}$ , is below the unidirectional noise. This extrapolation must be confirmed with realistic data on fiber losses and on submarine amplifier's gain. The cumulative spontaneous emission of the optical amplifiers (up to 75) can be the limiting factor of such a method.

Finally we evaluate the accuracy of the frequency comparison. We calculate the mean value of the beat note frequencies recorded with a  $\Pi$ -type counter and its standard deviation for consecutive segments from 1 to 1000 s [12]. For the bidirectional setup, with the set of 138 000 data of 1 s of Fig. 2, the mean offset frequency is  $7 \times 10^{-21}$ . The statistical relative uncertainty of the mean value, calculated as the relative

standard deviation divided by the length of the consecutive segment, has a constant value of  $3 \times 10^{-21}$  as expected for white phase noise [25]. For longer segments, this value slightly increases, due to long-term Flicker noise. We finally set a conservative estimate of the statistical fractional uncertainty of the frequency comparison as the long-term overlapping Allan deviation of the data set, which is  $2 \times 10^{-20}$  at 20 000 s integration time. For the two-way unidirectional, using 160 000 data of 1 s of the remote comparison, we find a relative mean offset frequency of  $8 \times 10^{-18}$  with a statistical fractional uncertainty of  $6.5 \times 10^{-17}$  given by the overlapping Allan deviation at 40 000 s integration time. This demonstrates that the frequency comparison shows no deviation to the expected value.

We have demonstrated two setups able to compare optical frequencies between two distant laboratories at ultrahigh resolution and short averaging time on a 100-km telecommunication network. The first setup uses two fibers for each propagation way and comply with unidirectional amplifiers used in telecommunication networks. It can be easily implemented over a telecommunication network under operation, as long as the switches and routers are bypassed. We demonstrated a frequency comparison with a relative frequency stability of  $2 \times 10^{-17}$  at 40 000 s integration time in a 1 Hz bandwidth. This two-way unidirectional method gives the possibility to perform measurements *in situ* and in real time. It opens the way to intercontinental clocks comparison with fiber links in parallel with data traffic at a level of resolution and accuracy competitive with the most advanced satellite techniques and with much shorter integration time. The second two-way setup uses bidirectional frequency transfer in a single fiber. It gives the possibility to perform accurate and high-resolution frequency comparison with simple electronics, with an outstanding relative stability of  $5 \times 10^{-21}$  at 4 000 s integration time.

The authors thank Giorgio Santarelli for helpful and stimulating discussions. They also thank Emilie Camisard, Thierry Bono, and Patrick Donath at the GIP Renater; François Biraben, François Nez, and Saïda Guellati-Khelifa at Laboratoire Kastler-Brossel; and Christian Hascoet and his team at Information Technologies Department at Pierre-et-Marie-Curie University (UPMC) for giving them the opportunity to use the different spans of the fiber's loop. This work is supported by the European Metrology Research Programme (EMRP) under SIB-02 NEAT-FT. The EMRP is jointly funded by the EMRP participating countries within EURAMET and the European Union. This work is supported by the E.U. under GN3+, the Labex FIRST-TF, the French spatial agency CNES, IFRAF-Conseil Régional Ile-de-France, and Agence Nationale de la Recherche (Grant No. ANR-2011-BS04-009-01).

- 
- [1] F. R. Giorgetta, W. C. Swann, L. C. Sinclair, E. Baumann, I. Coddington, and N. R. Newbury, *Nat. Photonics* **7**, 434 (2013).  
 [2] B. J. Bloom, T. L. Nicholson, J. R. Williams, S. L. Campbell, M. Bishof, X. Zhang, W. Zhang, S. L. Bromley, and J. Ye, *Nature (London)* **506**, 71 (2014).

- [3] T. Kessler, C. Hagemann, C. Grebing, T. Legero, U. Sterr, F. Riehle, M. J. Martin, L. Chen, and J. Ye, *Nat. Photonics* **6**, 687 (2012).  
 [4] M. Fujieda, D. Piester, T. Gotoh, J. Becker, M. Aida, and A. Bauch, *Metrologia* **51**, 253 (2014).

- [5] N. R. Newbury, P. A. Williams, and W. C. Swann, *Opt. Lett.* **32**, 3056 (2007).
- [6] M. Fujieda, M. Kumagai, S. Nagano, A. Yamaguchi, H. Hachisu, and T. Ido, *Opt. Express* **19**, 16498 (2011).
- [7] K. Predehl, G. Grosche, S. M. F. Raupach, S. Droste, O. Terra, J. Alnis, T. Legero, T. W. Hänsch, T. Udem, R. Holzwarth, and H. Schnatz, *Science* **336**, 441 (2012).
- [8] O. Lopez, A. Haboucha, B. Chanteau, C. Chardonnet, A. Amy-Klein, and G. Santarelli, *Opt. Express* **20**, 23518 (2012).
- [9] P. Krehlik, L. Sliwczynski, L. Buczek, and M. Lipinski, *IEEE Trans. Instrum. Meas.* **61**, 2844 (2012).
- [10] D. Calonico, E. K. Bertacco, C. E. Calosso, C. Clivati, G. A. Costanzo, M. Frittelli, A. Godone, A. Mura, N. Poli, D. V. Sutyryn, G. Tino, M. E. Zucco, and F. Levi, *Appl. Phys. B* **117**, 979 (2014).
- [11] G. Marra, H. S. Margolis, and D. J. Richardson, *Opt. Express* **20**, 1775 (2012).
- [12] S. Droste, F. Ozimek, T. Udem, K. Predehl, T. W. Hänsch, H. Schnatz, G. Grosche, and R. Holzwarth, *Phys. Rev. Lett.* **111**, 110801 (2013).
- [13] F. Kéfélian, O. Lopez, H. Jiang, C. Chardonnet, A. Amy-Klein, and G. Santarelli, *Opt. Lett.* **34**, 1573 (2009).
- [14] O. Lopez, A. Kanj, P.-E. Pottie, D. Rovera, J. Achkar, C. Chardonnet, A. Amy-Klein, and G. Santarelli, *Appl. Phys. B* **110**, 3 (2013).
- [15] D. W. Hanson, *Proceedings of 43rd Annual Symposium on Frequency Control, Denver, CO* (IEEE, Piscataway, NJ, 1989), pp. 174–178.
- [16] S. Raupach, H. Schnatz, G. Grosche, and S. Droste, *Proceedings of the European Frequency and Time Forum, Gothenburg, Sweden* (IEEE, Piscataway, NJ, 2012), pp. 161–162.
- [17] C. E. Calosso, E. Bertacco, D. Calonico, C. Clivati, G. A. Costanzo, M. Frittelli, F. Levi, A. Mura, and A. Godone, *Opt. Lett.* **39**, 1177 (2014).
- [18] P. A. Williams, W. C. Swann, and N. R. Newbury, *J. Opt. Soc. Am. B* **25**, 1284 (2008).
- [19] S. Dawkins, J. McFerran, and A. Luiten, *IEEE Trans. Ultrason. Ferroelectr. Freq. Control* **54**, 918 (2007).
- [20] A. Bercy, S. Guellati-Khelifa, F. Stefani, G. Santarelli, C. Chardonnet, P.-E. Pottie, O. Lopez, and A. Amy-Klein, *J. Opt. Soc. Am. B* **31**, 678 (2014).
- [21] L. S. Ma, P. Jungner, J. Ye, and J. L. Hall, *Opt. Lett.* **19**, 1777 (1994).
- [22] H. Jiang, F. Kéfélian, S. Crane, O. Lopez, M. Lours, J. Millo, D. Holleville, P. Lemonde, C. Chardonnet, A. Amy-Klein, and G. Santarelli, *J. Opt. Soc. Am. B* **25**, 2029 (2008).
- [23] F. Stefani, O. Lopez, A. Bercy, W.-K. Lee, C. Chardonnet, G. Santarelli, P.-E. Pottie, and A. Amy-Klein, [arXiv:1412.2496](https://arxiv.org/abs/1412.2496).
- [24] S.-C. Ebenhag, P. O. Hedekvist, and K. Jaldehag, *Proceedings of the 43rd Annual Precise Time and Time Interval Systems and Applications Meeting* (Long Beach, CA, 2011), pp. 9–16.
- [25] W.-K. Lee, D.-H. Yu, C. Y. Park, and J. Mun, *Metrologia* **47**, 24 (2010).